Microelectromechanical Systems (MEMS) Actuated Wave Front Correcting Subreflector: Distortion Compensation for Large Reflector Antennas

William A. Imbriale[(1)], Yahya Rahmat-Samii[(2)], Harish Rajagopalan[(2)] Shenheng Xu[(2)] and Vahraz Jamnejad[(1)]
(1) Jet Propulsion Laboratory, California Institute of Technology
Pasadena, CA 91109
(2) Department of Electrical Engineering, University of California, Los Angeles
Los Angeles, CA 90095

***Abstract*-Gain loss in large reflector antennas due to main reflector surface distortion is a significant problem in both ground and spacecraft antennas. There are two aspects that need to be considered: 1) Since the shape of the main reflector surface is generally not known it is necessary to determine the characteristics of the actual distortion in real time and 2) A method of compensating for the distortions is required.**

Three techniques for measuring the main reflector surface distortion are discussed. 1) A two-camera optical surface-measuring system using photogrammetry, 2) A small array feed placed in the focal plane of the reflector system and 3) Small probes placed on the subreflector. It was demonstrated that all three methods can recover the main reflector distortion with the subreflector probe method seeming to offer the simplest (least number of probes and minimal computation) implementation.

Extensive work has been performed at JPL on the use of a deformable mirror to correct for the gravity induced distortions on a large ground reflector antenna. This work culminated in a demonstration of a deformable mirror on the NASA/JPL 70-meter antenna in early 1999. An electronic version of the deformable mirror is proposed for use with large reflector inflatable antennas for spacecraft. The mirror consists of a light weight surface made up of a reflect array of patches whose reflection phase is controlled via RF MEMS switches. Different reflectarray designs were studied for this particular application and it was decided that the element with variable slot on the ground plane was best suited keeping in mind the MEMS implementation. Some experimental results with the MEMS integrated with the reflect array patch are shown.

I. INTRODUCTION

In recent years, advanced spaceborne applications have imposd stringent requirements on large reflector antennas. To meet the great challenge of ever-increasing reflector size and limited space and weight in spaceborne applications, deployable reflector antennas such as mesh reflector antennas and inflatable membrane antennas [1]–[3] have been proposed due to their inherent advantages of being lightweight, small in size before deployment, and reasonable production cost. However, reflector surface distortions are inevitable either due to manufacturing errors, initial on-orbit deployment errors, long term changes in material properties or thermal effects. Therefore, distortion compensation of one form or another is necessary to overcome the resultant performance degradation.

This paper discusses a unique technique for distortion compensation using a wave front correcting subreflector consisting of reflectarray patches whose phase reflection properties are controlled through the use of MEMS switches. One of the difficulties of applying this or any other technique for compensating spacecraft reflector antenna distortions is that the shape of the surface is typically unknown and changes with time. Therefore, some methodology for determining the reflector shape in real time is required. This paper also proposes three techniques that can provide a real time estimate of main reflector shape.

II. REAL TIME ESTIMATE OF REFLECTOR DISTORTIONS

Three algorithms for main reflector surface determination were studied: 1) A two-camera optical surface-measuring system using photogrammetry, 2) A small array feed placed in the focal plane of the reflector system and 3) Small probes placed on the subreflector. It was demonstrated that all three methods can recover the main reflector distortion, however the subreflector probe method seems to offer the simplest (least number of probes and minimal computation) implementation.

Photogrammetry: Photogrammetry is a remote sensing technology in which geometric properties about objects are determined from photographic images. In the simplest example, the three-dimensional coordinates of points on an object are determined by measurements made in two or more photographic images taken from different positions. Common points are identified on each image. A line of sight (or ray) can be constructed from the camera location to the point on the object. It is the intersection of these rays (triangulation) that determines the three-dimensional location of the point. Using special targets mounted on the main reflector surface, and two cameras mounted on booms, simultaneous digital images are acquired and processed to provide the surface shape. An example for a 6-meter ground measured to provide

surface distortion as a function of sun illumination is given in reference [4].

Array feed: For this application, a small array feed is placed at the focal plane of the reflector system. The amplitude and phase received at each element of the array feed can be used to compute the main reflector distortion. The solution is as follows: From the signals received at the array feed estimate the Focal Plane Fields and then use the Focal Plane Fields compute the reflector distortion.

To solve for the Focal plane fields, postulate a Fourier series representation of the Focal Plane Field with unknown coefficients $C_{nm.}$ Then convolve the Focal plane fields with the feed aperture distribution to write an expression for the feed response in terms of the unknown coefficients. Using the measured feed response, solve for the coefficients using least squares as a maximum likelihood indicator. This gives an estimate of the Focal plane fields. Conjugate the Focal Plane fields and then propagate them to the main reflector in the undistorted system. Estimate the surface distortion by differing the phase from these fields to the fields computed from an undistorted system (determines negative surface).

Subreflector probes: For this method, the phase at a selected number of points on the subreflector is measured through the use of a small number of receiving patch elements (probes). By probing the phase change at a few selected positions on the subreflector, the full range of phase error can be recovered and subsequently used to change the phase of all the patch elements covering the subreflector plane to compensate for the main reflector errors. This is accomplished by using a version of the circular sampling theorem. The sampling is performed on the phase error function on the circular aperture of the main reflector. Expanding this function in a Zernike polynomial set [5] and building upon the theory first applied to the reflector aperture integration [6-7], a sampling method is derived which provides an exact retrieval of the coefficients of up to certain orders by a corresponding set of selected points in the ρ, ϕ directions. Once these points are identified, corresponding points on subreflector are obtained. A probing of the fields at these points results in a set of phase values that are then transferred back to the main reflector aperture for recovering the phase function. Once this function is recovered, the corresponding phase values at all the points on the subreflector are calculated and can be applied to the array of phase shifting patch elements to compensate for aperture or surface errors. The details are given in reference [8] and only a representative example is given here.

The geometry is shown in Figure 1. The use of 21 probes was selected as an example, which is capable of replicating a distortion up to 4 radial and 4 azimuthal terms in the Zernike polynomial expansion of the surface error. The selected sampling points in the main reflector are shown in Figure 2 with the corresponding points mapped to the subreflector shown in Figure 3. As an example of a possible phase distortion, the function $\Delta z = \varepsilon\rho^3 \cos(3\varphi)$ is considered. This is Zernike function of serial order 10 (m = 3, n = -3) as shown in Fig. 4. The coefficient $\varepsilon = 0.2\ \lambda$ results in a loss of about 3.4 dB.

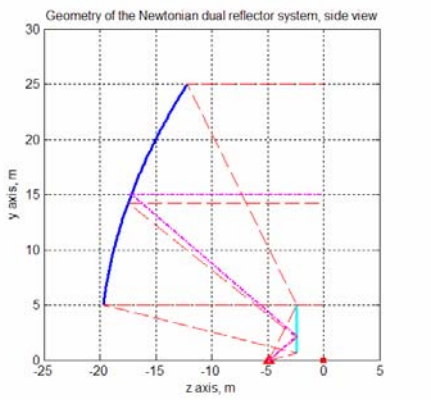

Fig. 1. Geometry of a Newtonian dual reflector used for the example

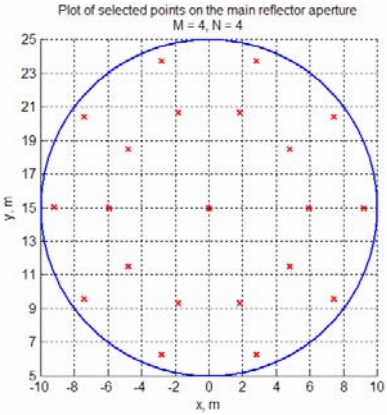

Fig. 2. Plot of selected points on the main reflector

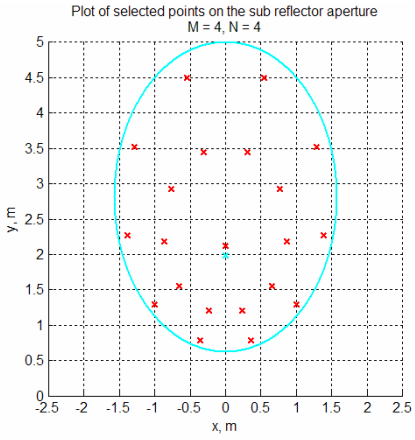

Fig. 3. Plot of corresponding points on the subreflector

By using sample values at locations given in Fig. 2 with appropriate weights, the original function can be exactly recovered. Using Physical Optics (PO) and the Physical Theory of Diffraction (PTD), the phase of the corresponding sample points on the subreflector are shown in Fig. 5. Using the phase at these points (the subreflector probes) on the subreflector, using geometric optics (GO) to propagate the

errors to the main reflector, and applying the sampling theorem results in the reconstructed error function shown in Figure 6.

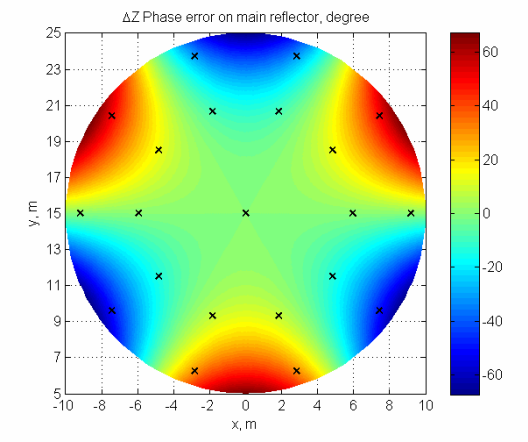

Fig. 4. Δz phase error on the main reflector

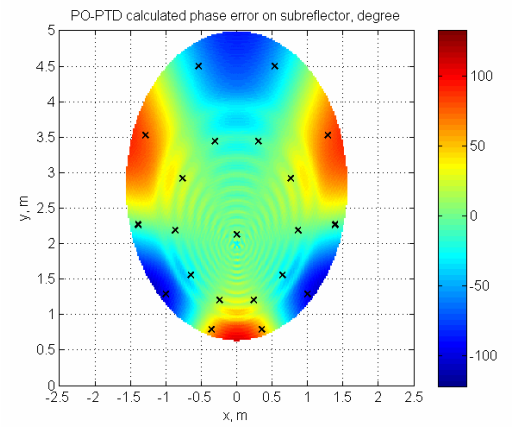

Fig. 5. PO-PTD calculated subreflector phase error

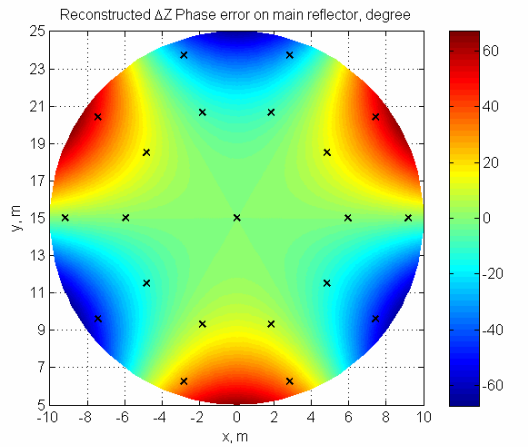

Fig. 6. Recovered reflector phase error on main reflector

III. Distortion Compensation

Extensive work has been performed at JPL on the use of a deformable mirror to correct for the gravity induced distortions on a large ground reflector antenna. This work culminated in a demonstration of a deformable mirror on the NASA/JPL 70-meter antenna in early 1999 [9]. An electronic version of the deformable mirror is proposed for use with large reflector inflatable antennas for spacecraft. The mirror would consist of a light weight surface made up of a reflectarray of patches whose reflection phase is controlled via RF MEMS switches. A microstrip reflectarray is a low profile, inexpensive antenna that combines some of the best features of reflectors and microstrip arrays. The critical feature of the reflectarray implementation is that the individual element is capable of scattering the incident field with the pre designated phase.

This section demonstrates the concept of using a reflectarray to compensate for main reflector distortions. In this example, a variable size patch element is used to generate the required phase reflection. The following section demonstrates the use of MEMS switches to control the phase.

To compute this example, a reflectarray code was integrated with a physical optics (PO) reflector code. The example chosen was a circularly symmetric reflector with diameter D = 5 meters, F/D = 1.0, Frequency = 13.285 GHz and distortion of $\Delta z = \varepsilon\rho^2\cos(2\varphi)$ with ε = 7.5 mm. The feed has a $\cos^n(\theta)$ pattern with n=11.82. The computed patterns are shown in Figure 7. Figure 7a shows the result with a reflectarray chosen to simulate a flat plate with zero main reflector distortion, figure 7b the result with a simulated flat plate and distorted main reflector and figure 7c the result with the distorted main reflector and the compensating reflectarray. The required phase shift was obtained using the conjugate phase method and the variable phase shift from the reflectarray obtained by variable size patches as shown in Figures 8 and 9. Further details and examples can be found in reference [10].

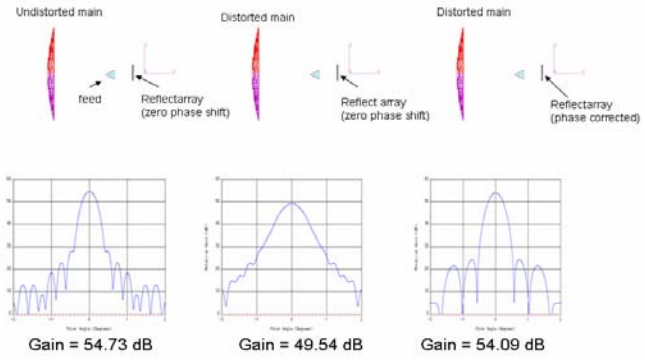

Fig. 7. Phase correcting reflectarray

IV. Use Of MEMS Switches To Provide The Variable Phase Shift

The reconfigurable reflectarray element is designed using commercially available Radio Frequency Micro-Electromechanical System (RF MEMS) switches. The element consists of a microstrip patch on the top surface and a

slot with an actuated variable length in the ground plane. RF MEMS switches are mounted on the slot to electronically vary the slot length by actuating the switches and thus obtaining the desired phase response. Waveguide measurements and High Frequency Structure Simulator (HFSS) simulations are used to characterize the reflectarray element.

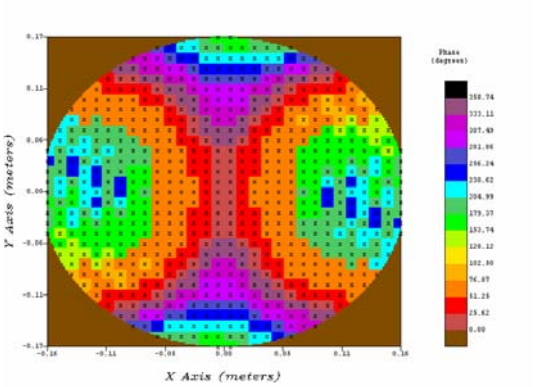

Fig. 8. Required phase shift computed by conjugate phase method

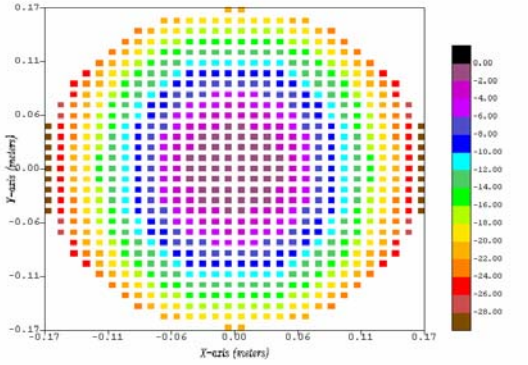

Fig. 9. Patch Array - Phase shift by unequal patch size

Various potential reflectarray element designs were considered, which included variable size patches, patches with variable length slot, and patches with fixed slot fed by variable length stripline. After detailed study and systematic evaluation, it was decided that the reflectarray element with the patch on the top surface and the variable length slot in the ground plane was best suited by taking into consideration the eventual implementation of MEMS technology for this study. The primary advantage of such a reflectarray is that the MEMS switches, the DC biasing wires, and the control circuitry will be on the backside of the reflectarray, and there will be no electronics on the top surface (the re-radiating surface) of the reflectarray design.

Radant MEMS SPST-RMSW100 electrostatic switches were used for achieving reconfigurability. These switches are electrostatically actuated cantilever beams connected in a three-terminal configuration. When a DC bias voltage is applied between the gate and the source, an electrostatic force results, which deflects the beam toward the substrate and turns on the switch. The actuation voltage for the switch is 90 VDC applied between the gate and the source. The insertion loss of 0.15 dB, return loss of 25 dB, and isolation of 20 dB was measured at 2 GHz for the RF MEMS switch. As mentioned in [11], in the actuated state, the device behaves as a 50 Ω microstrip transmission line, and in the open state the device appears largely capacitive.

The three terminals (gate, source, and drain) compose the inputs and outputs into the hermetically sealed switch package which is fabricated on a grounded silicon substrate. The packaged switch has overall outer dimensions of 1.45 mm x 1.45 mm x 0.25 mm. The RF MEMS switch has a gold base. Copper pads of dimensions 1.45 mm x 1.45 mm (similar to switch dimensions) were etched on the slot, as shown in Fig. 10(a). This way the gold on the bottom of the switch could directly be glued using conductive epoxy to the copper pads; thus the gold base does not need to be polished off [12]. HFSS simulations showed that, with the addition of copper pads on the slot, the reflection phase results were similar to the case when the pads were not present. Fig. 10(b) shows the RF MEMS switches glued onto the copper pads and wire bonded to the substrate. The source and drain terminals of the switch are wire bonded (1 mil diameter aluminum wire) across the slot with two wire bonds each, and the gate terminal is wire bonded to the DC isolation layer that is glued to the back end of the ground plane. Fig. 11 shows the back surface of the reflectarray element with the MEMS switches glued to the slot, the wire bonds, the isolation layer, and the DC bias lines. The microstrip patch is on the top surface of the reflectarray element. Fig. 12 shows the measurement setup. S-band waveguide with a flange is used for the reflection phase and S11 measurements. Using 4 switches we get 10 distinct states (4 from symmetric and 6 from asymmetric loading). Using both symmetric and asymmetric loading allows for 10 independent states and provides better phase quantization. The measurements show that a total phase shift of 150° is obtained for the current design with a maximum loss of about 1.5 dB.

Table I shows the measurement results for both S_{11} and reflection phase for the possible 10 states. The reflection phase results provided in Table I are the phase values at the top surface of the patch. For the application of main reflector surface distortion compensation, these reflection phase values are the same as the transmission phase of the wave reflected by the reflectarray (subreflector) onto the main dish. It should be noted that when more MEMS switches are mounted on the slot, bigger phase swing is possible. Further details can be found in reference [13].

V. CONCLUSIONS

A novel technique for compensating the effects of main reflector distortion consisting of MEMS switches integrated into patch reflectarray elements of a subreflector has been presented. In addition, techniques for providing a real time estimate of the required distortion were presented. Taken together, this technology provides a methodology for improving the performance of large spacecraft antennas.

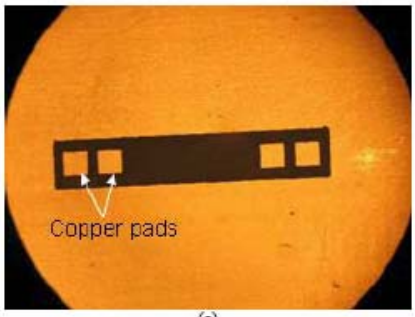

(a)

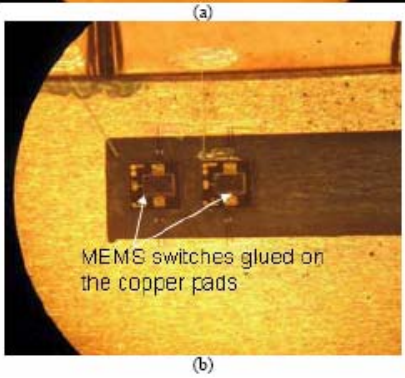

(b)

Fig. 10. (a) Copper pads etched on the slot. (b) RF MEMS switches mounted on the copper pads on the slot.

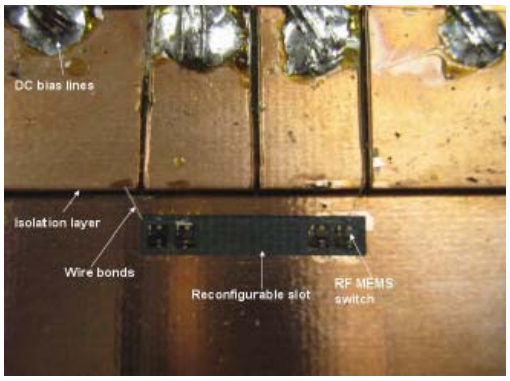

Fig. 11. The reconfigurable slot with four RF MEMS switches mounted.

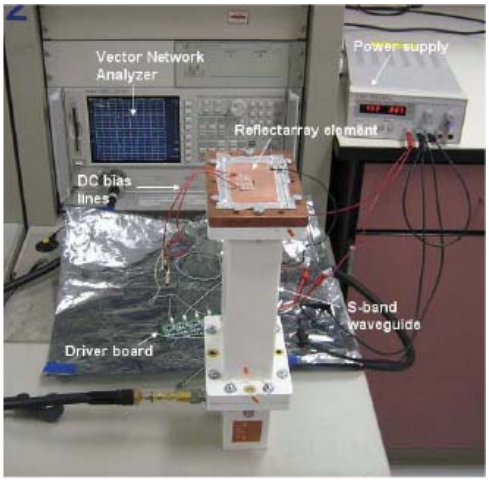

Fig. 12. The measurement setup using S-band waveguide and specially designed waveguide fixture.

TABLE I
S_{11} and reflection phase measurement results for the 10 distinct states.

Loading S - symmetric A - asymmetric	Switch State	Measurement S11(dB)	Measurement Phase (deg)
S	0	-0.47	-132.75
A	1,8	-0.64	-115.95
S	9	-0.89	-94.33
A	2,4	-0.93	-91.81
A	3,12	-1.05	-79.09
A	5,10	-1.31	-57.81
A	11,13	-1.41	-43.92
S	6	-1.57	-17.23
A	7,14	-1.58	1.04
S	15	-1.52	15.47

ACKNOWLEDGMENT

The research was carried out at the Jet Propulsion Laboratory, California Institute of Technology, under a contract with the National Aeronautics and Space Administration.

REFERENCES

[1] A. G. Roederer and Y. Rahmat-Samii, "Unfurable satellite antennas: A review," Annales des Telecommunications, vol. 44, no. 6–10, pp. 475–488, Nov. 1989.

[2] C. G. Cassapakis, A. W. Love, and A. L. Palisoc, "Inflatable space antenna: A brief review," Proc. 1998 IEEE Aero. Conf., vol. 3, pp. 453–459, 1998.

[3] E. G. Njoku, Y. Rahmat-Samii, J. Sercel, W. J. Wilson, and M. Moghaddam, "Evaluation of an inflatable antenna concept for microwave sensing of soil moisture and ocean salinity," IEEE Trans. Geosci. Remote Sens., vol. 37, no. 1, pp. 63–78, Jan. 1999.

[4] W. A. Imbriale, E. Gama, K. S. Smith, and R. Shultz, "Thermal Considerations for Hydroformed Reflectors," 2006 IEEE Aerospace Conference, Big Sky Montana, March 2006.

[5] M. Born, E. wolf, *Principles of Optics,* New York: Pergamon Press, pp. 464-466 and 767-772, 1980.

[6] V. Jamnejad, "A New Look at the Circle Polynomial Series Representation of the Radiation Integral of Reflector Antennas," AP-S International Symposium Digest, Vol. 1, pp. 309-313, June 1984.

[7] V. Jamnejad, "A New Integration Scheme for Application to the Analysis of Reflector Antennas," AP-S International Symposium Digest, Vol. 1, pp. 380-384, June 1984.

[8] V. Jamnejad and W. Imbriale, "On Reflector Surface Compensation by Probing the Subreflector Field in Dual Reflector Antennas," 29th ESA Antenna Workshop on Multiple Beams and Reconfigurable Antennas, Noordwijk, The Netherlands, April 2007.

[9] W. A. Imbriale, *Large Antennas of the Deep Space Network*, John Wiley & Sons, Inc., Hoboken, New Jersey, 2003.

[10] S. Xu, H. Rajagopalan, Y. Rahmat-Samii, and W. A. Imbriale, "A Novel Reflector Surface Distortion Compensating Technique Using a Sub-Reflectarray," Proc. IEEE Ant. and Prop. Symposium, pp. 5315–5318, June 2007.

[11] [Online]. Available: http://www.radantmems.com.

[12] G. H. Huff and J. T. Bernhard, “Integration of packaged RF MEMS switches with radiation pattern reconfigurable square spiral microstrip antennas,” IEEE Trans. Antennas Propag., vol. 54, pp. 464–469, Feb. 2006.
[13] H. Rajagopalan, Y. Rahmat-Samii, and W. A. Imbriale, “RF MEMS Actuated Reconfigurable Reflectarray Patch-Slot Element,” Submitted to the IEEE Transactions on Antennas and Propagation.